Cellulosic surfaces endowed with chemical reactivity by physical adsorption of functionalized polysaccharides

Arthur Bouchut, Bernard Cathala, Céline Moreau, Michael Lecourt, Michel Petit-Conil, Asja Pettignano, Julien Bernard, Aurélia Charlot, Etienne Fleury

▶ **To cite this version:**

Arthur Bouchut, Bernard Cathala, Céline Moreau, Michael Lecourt, Michel Petit-Conil, et al.. Cellulosic surfaces endowed with chemical reactivity by physical adsorption of functionalized polysaccharides. Cellulose, 2023, 30 (13), pp.8185-8203. 10.1007/s10570-023-05283-9 . hal-04256011

HAL Id: hal-04256011
https://hal.science/hal-04256011v1

Submitted on 24 Oct 2023

HAL is a multi-disciplinary open access archive for the deposit and dissemination of scientific research documents, whether they are published or not. The documents may come from teaching and research institutions in France or abroad, or from public or private research centers.

L'archive ouverte pluridisciplinaire **HAL**, est destinée au dépôt et à la diffusion de documents scientifiques de niveau recherche, publiés ou non, émanant des établissements d'enseignement et de recherche français ou étrangers, des laboratoires publics ou privés.

Cellulosic surfaces endowed with chemical reactivity by physical adsorption of functionalized polysaccharides

Arthur Bouchut[1], Bernard Cathala[2], Céline Moreau[2], Michael Lecourt[3], Michel Petit-Conil[3], Asja Pettignano[1], Julien Bernard[1], Aurélia Charlot[1], Etienne Fleury[1]*

[1] Université de Lyon, INSA LYON, Ingénierie des Matériaux, Polymères IMP-UMR CNRS 5223 F 69621, Villeurbanne, France

[2] UR 1268 Biopolymères, Interactions et Assemblages, INRA, F-44316, Nantes

[3] InTech Fibres Division, FCBA, Domaine Universitaire, CS 90252, 39044 Grenoble Cedex 9, France

*Corresponding authors: aurelia.charlot@insa-lyon.fr

KEYWORDS

ABSTRACT

A strategy to modify cellulosic surfaces through the physical adsorption of xyloglucan (XG) and carboxymethyl cellulose (CMC) derivatives bearing allyl or alkyne functions was investigated. The grafting reaction trough epoxide opening of allyl glycidyl ether (AGE) or propargyl glycidyl ether (PGE) in mild basic aqueous medium conditions was deeply explored and the chemical structure was evidenced by combining FTIR, Raman and NMR techniques. A set of derivatives having a degree of substitution -DS- ranging from 0.4 to 0.44 was prepared. Allyl-XG and -CMC derivatives were engaged with success in radical polymerization in aqueous medium giving hydrogels with various swelling properties. The

deposition of polysaccharides derivatives onto Whatman paper and wood pine fibers was evaluated by titration and result disclosed that neither the nature of grafting moieties nor the DS alter their deposition. QCM-D measurements have stated interactions between polysaccharides derivatives and cellulose surface confirming the ability of Allyl-XG to well adsorb. Topochemical mapping by confocal Raman with alkyne derivatives highlighted that the covering is complete and that the diffusion inside the cellulosic substrate reach 40 μm. This strategy allows for tuning the adhesion of the layers and its reactivity towards top-coats.

1. Introduction

It is now well established that the depletion of fossil resources requires innovative alternative sustainable solutions in diverse areas of economic activities [1]. In this context, cellulosic materials are key and inescapable substrates for the present and future development of high-performance green materials [2]. Cellulosic substrates can be found under different shapes and compositions depending on their origin, their refining level and also on the specific applied treatments such as partial oxidation. Cellulosic substrates can be employed in a wide range of current applications from paper [3] to textile [4] but also in order to design new advanced materials such as composites [5], conductive fillers [6] or medical devices with nanocellulose fibers [7]. A crucial point with cellulosic materials lies in the tunability of their chemical and physical surface features, allowed for example by covalent grafting with (macro)molecules [8] mainly according “grafting from” or “grafting onto” strategies [9]. These covalent surface modification routes offer many advantages, notably linked to the large diversity of species amenable to be grafted and to the strength of the covalent bond enhancing the durability of the functionalized cellulose materials. However, when harsh experimental reaction conditions are employed, the attributes of cellulose in terms of crystallinity and mechanical properties for instance can be affected and/or cellulose can be subjected to a structural alteration [9, 10]. Also, grafting approaches are not so versatile and the chemical

process has to be readapted to the substituent used for the ligation. Consequently, covering cellulosic materials with appropriated coatings is commonly exploited for industrial applications [11]. As an example, wood panels are often coated by acrylate monomers able to polymerize upon UV irradiation, but the poor chemical affinity at the interface between the cross-linked coating and the cellulosic substrate may create a weakening of adhesion, which considerably impedes the durability of the performance of the material [12].

In order to alleviate these concerns, an alternative strategy to tailor the surface properties of cellulosic substrates consists in the physical adsorption of judiciously chosen polymers exhibiting good chemical affinities for cellulose [13, 14, 15, 16]. The interest is thus to modulate the surface properties of cellulose in mild conditions without having any detrimental effect regarding its native appealing advantages. Such approach is particularly attractive from the sustainability point of view, since the deposition process can be carried out from aqueous solutions and it results from the formation of non-covalent interactions at the interface which presents some assets in terms of reversibility and recyclability.

As most of cellulosic substrates are negatively charged due to the presence of hemicelluloses and/or carboxylic groups onto cellulose backbone, cationic polymers make them ideal candidates because of the entropy increase consecutive to the counter-anion release [16]. Examples of cationic polymers adsorption onto cellulosic substrates are numerous and range from starch [17] to xylans [18] used in paper manufacture to chitosan [20] and cationized polyacrylate latex [20] or even more complex functional materials such as positively charged polymeric nanoparticles generated by polymerization induced self-assembly [21]. Polyanions, such as carboxymethylcellulose (CMC) were also exploited with these anionic substrates. Indeed, even though CMC cannot be adsorbed onto cellulosic surfaces at low salt concentrations due to electrostatic repulsions, the use of high concentration of salt: sodium, magnesium, calcium… allows it [13]. Filpponen *et al*. reported on the adsorption of azide- or

alkyne-modified CMC onto amorphous cellulose able to further react with alkyne-modified bovine serum albumin BSA or azide containing methoxy-poly(ethylene glycol). The authors claimed a new concept consisting in sequentially combining the robust physical adsorption ("physical click") followed by robust chemical reaction ("chemical click") [16]. The adsorption phenomenon can also be modulated by playing with the hydrophophilic-hydrophobic balance of the polyelectrolyte. This strategy was described by Grigoray *et al.* [22] who designed water-soluble photo-responsive cellulose derivative capable to adsorb onto cellulosic fibers. The adsorption was then monitored by adjusting the balance between the polymer-solvent interaction χ and the polymer-surface interaction χ_s. Moreover, we recently demonstrated that partially hydrophobized CMCs by Passerini three-component reaction can be greatly adsorbed onto cellulose surfaces [23]. Non-ionic polymers and in particular non-ionic polysaccharides from the lignocellulosic biomass can also be adsorbed onto cellulose surfaces as described for xylans [24], arabinoxylans [25], or even mannan [26]. The adsorption not only depends on the propension of the polymer to develop hydrogen interactions at the interface but also on the conformation adopted by the chains, which is controlled by the overall hydrophilicity of the polymer. Thus, the composition of polysaccharides and in particular the nature of the substituents and the extent of the modifications are of great importance. Xylglucan (XG), a water-soluble polysaccharide mainly found in the cell wall of plants [27, 28], is another example whose high affinity for lignocellulosic surfaces is well documented [29, 30, 31, 32]. The adsorption results from an entropy-driven process. Whereas the xyloglucan composition has low effect on its capability to interact with cellulosic surfaces [33, 34], its molecular weight closely dictates the conformation of the XG chains deposited onto the substrate and highly impacts the yield of physisorption [35, 36]. For these reasons, chemically modified XG derivatives were deposited

onto cellulose surfaces, with the aim to impart cellulose with varied chemical functionalities, from chromophore to cationic species [15].

In the pursuit of the development of new ecodesigned cellulose material, we propose herein to endow cellulosic surfaces with chemical reactivity through the physical adsorption of xyloglucan (XG) and carboxymethyl cellulose (CMC) derivatives bearing allyl or alkyne functions. The final goal is to generate an intermediate layer strongly interacting with cellulosic surfaces and potentially able to chemically react with a top-coat (scheme 1). Such a never described modular platform, conjugating efficiency and sustainability, should allow for post-reactions of allyl functions according to various chemical routes such as thiol-ene [37, 38], hydrosilylation [39], radical reactions [40] and alkyne groups can be used in the well-known click chemistry [16, 41, 42] or can serve as specific tag [43].

Consistent with the use of bio-based polymers, the allyl and alkyne functions were introduced onto polysaccharide backbones by a simple and low environmental impact procedure involving an epoxide opening of allyl glycidyl ether (AGE) or propargyl glycidyl ether (PGE) in mild basic aqueous medium conditions. The functionalized polysaccharides (XG and CMC) were carefully characterized and their reactivity was evaluated in radical copolymerization in water medium. Then, their deposition onto cellulosic surfaces was examined and their propension to favorably interact together was finally investigated.

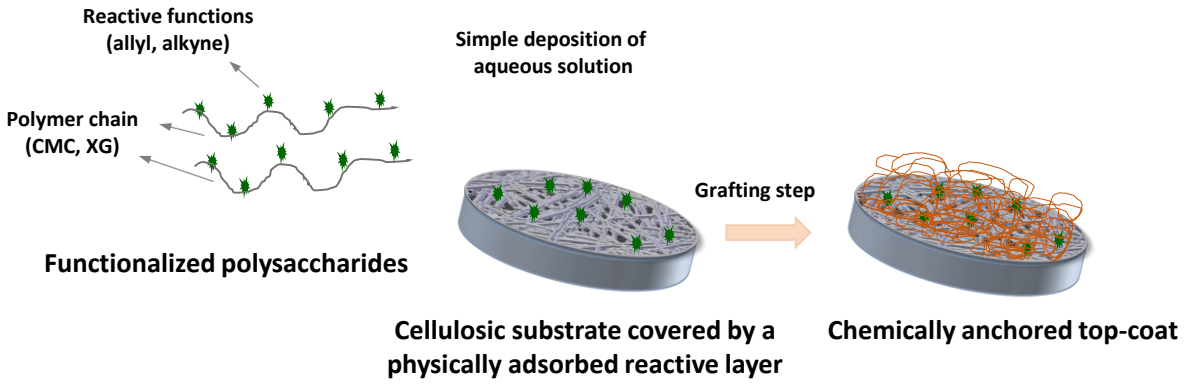

Scheme 1. Cellulosic substrates (paper, wood fibers) covered by an adsorbed layer made of chemically modified XG or CMC, able to further react with a reactive formulation

2. Experimental

2.1 Materials

Carboxymethyl cellulose sodium salt (NaCMC: CMC in the following text), having a degree of substitution of 0.7 (DS = average number of carboxymethyl groups per one anhydroglucose unit) and a Mw = 250,000 $g.mol^{-1}$, was provided by Sigma Aldrich. Xyloglucan was obtained from Megazyme with 95 wt% of purity, a molar mass Mw of 795,000 $g.mol^{-1}$ and composition, namely proportions of each unit given by the supplier are: Glucose 49 wt.%, Xylose 31 wt.%, Galactose 17 wt.% and 3 wt.% of other sugars. Cellulose substrates were cellulose Whatman and lignocellulosic fibers from maritime pine provided by the FCBA technology institute. The other chemicals were purchased from Sigma Aldrich (France) and used without further purification: propargyl glycidyl ether (PGE), allyl glycidyl ether (AGE), sodium hydroxide (≥98%), (+)-sodium (L)-ascorbate (≥99%), copper (II) sulfate (≥99%), acrylamide, sodium acrylate and sodium persulfate. The solvents were supplied by Carlo Erba.

2.2 Samples preparation

Xyloglucan and carboxymethyl cellulose functionalization with AGE or PGE

The functionalization of XG or CMC with AGE or PGE was performed in basic aqueous medium (through opening of the epoxy rings of AGE or PGE by the hydroxyl groups of the sugar). XG or CMC (200 mg) was solubilized in 20 mL of H_2O or H_2O/IPA (Isopropanol) solution (80/20 w/w, V = 20 mL). After complete dissolution of the polymer, NaOH pellets were added (from 0.33 to 3 eq/OH). The solution was then stirred for 30 min or until total

dissolution of NaOH. AGE or PGE (from 1 to 9 eq/OH) was then added to the solution and the vial was sealed. The reaction was carried for 7h at 60 °C under magnetic stirring. Then, the solution was slowly transferred to a cold IPA or acetone solution, in order to precipitate the polymer. The precipitate was then filtered using a Büchner (pore size 4) and washed several times with a solution of 20-30 mL of IPA or acetone. Then the precipitate was re-dissolved in a purely aqueous solution and re-precipitated under the same conditions to remove any trace of starting reagents. The precipitate was dissolved one last time in distilled water and freeze-dried to get white fluffy powder.

For allyl-functionalized derivatives, the DS were calculated by NMR after solubilization in D_2O (see below). For the alkyne-derivatives, polymers were first modified by "click" chemistry. For this purpose, 100 mg of product was dissolved in 20 mL of distilled water overnight. Sodium L-ascorbate and an azide molecule (11-Azido-3,6,9-trioxaundecan-1-amine, M = 218 g/mol) were added to the solution. The solution was then homogenized for 10 min under magnetic stirring, then $CuSO_4.5H_2O$ was introduced in solution. The quantities of each reagent are given by the following molar ratios: alkyne/azide/Cu^{2+}/ascorbate = 1/1/0.05/1, the number of alkyne functions being calculated with respect to the theoretical maximum DS (DS = 3). The solution was left under magnetic stirring at room temperature for 72 h. After reaction, the solution was dialyzed against water with a regenerated cellulose membrane (cut-off: 10 kDa) for 3 days to remove the catalyst and the excess of reagent. Finally, the dialyzed solution was freeze-dried and the DS_{alcyne} calculated from NMR analysis (see below).

Hydrogels preparation by radical copolymerization

The allyl- or alkyne-functionalized polysaccharide derivatives (m = 100 mg) were dissolved in 2.5 mL of distilled water at 70 °C. Then 0.5 mL of an aqueous solution containing 50 mg of

acrylamide and 50 mg of sodium acrylate was added. The total mass of polysaccharide derivatives and monomers corresponds to m_0. The solution was then degassed by bubbling argon for 30 min. Potassium persulfate (2 wt.%) was finally added to the medium in order to trigger the polymerization (and the formation of the hydrogel). The solution was maintained at 70 °C until gelation was macroscopically observed (usually after 15 min). The resulting hydrogel was immersed in 200 mL of distilled water for 24 h and the water was renewed several times to remove all unreacted products and was weighted for determining the mass m_s of the swollen hydrogel at equilibrium in water at 25°C. The hydrogel was finally freeze-dried in order to determine the mass m_d of the dry network corresponding to the mass of the reactants that have reacted. Extractable rate (T_{ex}.%) and swelling ratio (SR) were achieved from equation 1: $T_{ex}.\% = (m_0 - m_d)/m_0 \times 100$ and equation 2: $SR = (m_s - m_d)/m_d$ respectively.

2.3 Characterization

Raman analysis

Raman experiments were performed on a DXR Raman Microscope (ThermoFisher Scientific) equipped with an excitation wavelength at 532 nm and a 10 mW beam power. The spectra were collected using a 50 µm pinhole aperture and a polynomial fitting (at a polynomial order of 4) was used for fluorescence background correction. The Raman micrographs (1300 x 800 µm) were obtained from spectral data using point-by-point scanning with a 100 µm step size.

Nuclear Magnetic Resonance (NMR) spectroscopy

NMR experiments were recorded with Bruker Advance III 400 spectrometer (^{1}H: 400 MHz, 298 or 348 K, 64 and 1024 scans for molecules and macromolecules respectively; ^{13}C: 400 MHz, 348 K, 4096 to 8092 scans; HSQC and HMBC: 400 MHz, 348 K, 32-48 scans) with D_2O or DMSO-d6 as solvents. The chemical shifts (δ, ppm) are referenced to TSP-d4.

For the study of epoxide ring stability in aqueous solution by ^{1}H-NMR spectroscopy, the glycidyl ether, (AGE or PGE, C = 20-30 g.L^{-1}) was dissolved in a 1 mL volume of D_2O/IPA (80/20 w/w) solution. The onset of kinetics was marked upon the addition of NaOH (previously dissolved in D_2O/IPA) to reach a concentration of 0.05 mol/L. The solution was homogenized under magnetic stirring for a few seconds, then quickly transferred into an NMR tube (5 mm). The kinetics was then followed by ^{1}H-NMR at 60 °C and analyses were performed at defined times with 64 scans for each analysis. To investigate the kinetics of epoxide hydrolysis, proton integrals of the epoxide rings (at 2.78 and 2.97 ppm) were compared with those of the allyl (C***H*****$_2$**=CH-) or alkyne (-C***H*****$_2$**-C≡CH) functions for AGE or PGE (at 5.30 and 4.18 ppm respectively) which remain constant over time.

DS values were estimated from ^{1}H NMR spectra. For allyl-functionalized derivatives, the degrees of substitution (DS) were calculated from the integral of the anomeric protons I_{anomer} between 4.45 and 4.9 ppm and the one of one allyl proton I_{allyl} between 5.9 and 6.1 ppm, according the following equation: $DS_{allyl} = (I_{allyl})/(I_{anomer})$. For alkyne-functionalized derivatives, the degrees of substitution (DS) were calculated from the "clicked" derivatives as following $DS_{alkyne} = (I_{triazole})/(I_{anomer})$.

Deposition of polysaccharide derivatives and adsorption investigation

- Coating of cellulosic substrates by spraying (Scheme 2): an aqueous solution of polymer (5g.L^{-1}, pH 6) was sprayed onto cellulosic substrate (cellulose Whatman and wood fibers) and dried in an oven at 100 °C for 30 min in order to remove water and to favor adsorption of the polymer chains onto the substrate. The coated substrate was further immersed into distilled water solution to remove unbound chains (200 mL, 30 min). Through titration measurements, analyses of washing water allowed to quantitatively determine the amount of physisorbed polymers onto the substrate according this equation: $m_{adsorbed} = m_0 - (C_{aq} \times V_{aq})$ with m_0 the

mass of polymer sprayed on the substrate, C_{aq} the mass concentration of polymer in the washing water, measured by UV/Vis spectrometry according the Albalasmeh method (**SI.1**) and V_{aq} the volume of washing water. The adsorption yields were given by $m_{adsorbed}/m_0 x100$.

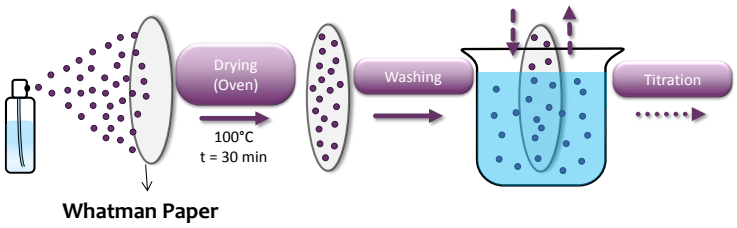

Scheme 2. Polymer adsorption onto Whatman paper by solution spraying/drying procedure

- **Analysis with Quartz Crystal Microbalance with Dissipation Monitoring (QCM-D)**

Adsorption Measurements were performed with a QCM-D E4 apparatus (Q-Sense, Sweden) equipped with 4 measuring cells (or modules). The QCM-D quartz crystals were coated with gold electrode on each side (QSX 301, Q-Sense, Sweden) and had a fundamental resonance frequency (f_0) of 5 MHz. The temperature of the QCM-D chamber was controlled at 20°C. Different cellulosic substrates were prepared from a coating onto commercially available gold quartz substrates (QSX 301, Q-Sense) previously cleaned in a Piranha bath (H_2SO_4: H_2O_2, 7: 3) rinsed thoroughly and dried under nitrogen flow before activation by a plasma treatment for 20 min. The first category of cellulosic substrate was obtained by firstly spin-coating of an aqueous solution of cationic poly(allyl amine) (C= 1 $g.L^{-1}$) onto gold sensor, which acts as an anchoring polymer to improve adsorption of cellulose onto the electrode surface (60 s of adsorption before rotation: 60 s, 3600 rpm, acceleration of 180 $rpm.s^{-1}$). Then, a second layer composed of cellulose nanocrystals (CNC) was spin-coated from a dispersion at 3 $g.L^{-1}$, before rotating the substrate (3000 rpm) for 60 s. CNC are derived from the acid hydrolysis of cotton linters. The conditions of hydrolysis are 64% H_2SO_4, 35 min at 65°C. The second category of cellulosic surfaces were obtained after the spin-coating of PAH (1 $g.L^{-1}$) onto the

gold sensor, and a second layer of amorphous cellulose was spin-coated (no adsorption before rotation: 180 s, 3600 rpm, acceleration of 180 rpm.s^{-1}) from a 5 g.L^{-1} solution in DMAc/LiCl [23]. After every layer was fabricated, the films were rinsed with water, by using the same spin-coating procedure employed for the two polymers. A final washing step was performed by immersing the surface in water, overnight, in order to ensure the complete removal of DMAc/LiCl. So, obtained surfaces were dried under nitrogen flow, followed by oven drying at 40 °C for 20 min, and stored in a desiccator until use. The thickness of the amorphous cellulose layer, measured by ellipsometry, was approximately 27 nm.

In the QCM-D cell, the PAH-NCC surfaces were treated by a continuous flow of water (100 µL.min^{-1}), allowing for reaching equilibrium at 20°C (i.e., when stable baselines for normalized frequency, $\Delta f_n/n$, and dissipation, ΔD_n, signals were obtained). The flow was then left at 50 µL.min^{-1} for 10 min. The solutions of polymers (15 □g.mL^{-1} in pure water at pH 7, filtered on a 5 □m cellulose nitrate filter) were then flowed for approximately 40 minutes. Finally, a rinsing step was performed by flushing the chamber with pure water solution, in order to remove the macromolecules that were loosely bound to the surface and verify the reversibility of the adsorption.

3. Results and discussion

Allyl and alkyne functionalization of xyloglucan and carboxymethylcellulose

The introduction of allyl and alkyne functions onto polysaccharides relies on epoxide-alcohol reaction between the hydroxyl groups of XG and CMC, and allyl glycidyl ether (AGE) or propargyl glycidyl ether (PGE), respectively. Such coupling involving allyl glycidyl ether was relatively well documented in the case of modification of starch [44], xylan [45], cellulose [46] and even CMC [47] but the use of propargyl glycidyl ether has scarcely been described [48]. By following well established procedure, the epoxide-alcool ligation was achieved in

aqueous basic medium [49]. As the epoxy rings can be subjected to non-desired hydrolysis which can compete with the etherification reaction, the stability of the glycidyl derivatives was monitored by ^{1}H-NMR analysis at 60°C in basic hydro-alcoholic conditions (details in experimental part).

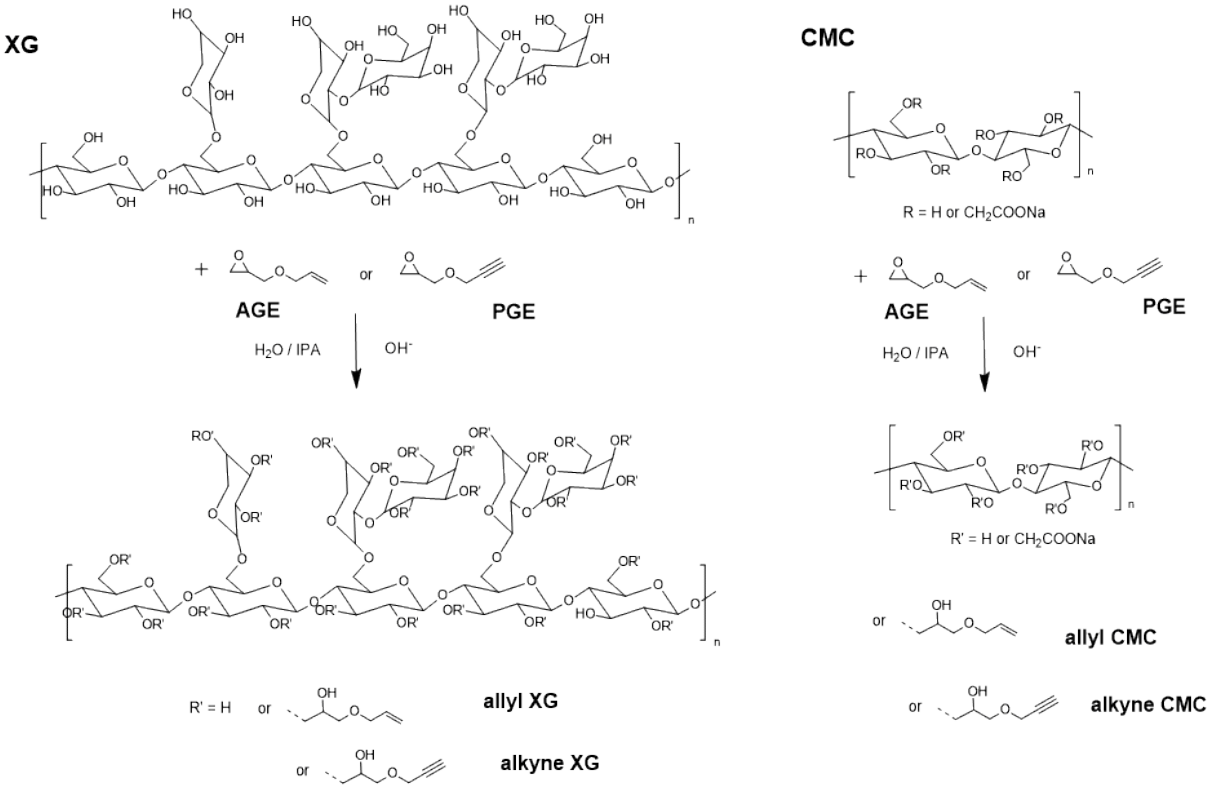

Scheme 3. Epoxide-alcool reaction between Xyloglucan (XG) or Carboxymethyl cellulose sodium salt (CMC) and propargyl glycidyl ether (PGE) or allyl glycidyl ether (AGE)

The comparison of the ^{1}H-NMR spectra of AGE in D_2O/IPA at 25°C (pH 6) (Figure 1.) shows a progressive decrease of the ^{1}H signals corresponding to the protons of the epoxide ring at 2.78, 2.97 ppm (a) and 3.35 ppm (b) over time. Concomitantly, multiple ^{1}H peaks gradually appear between 3.5 and 3.7 ppm, related to the formation of by-products such as glycerol 1-allyl ether and the dimer resulting from the coupling between AGE and glycerol 1-allyl ether (Figure **SI.2**). From equation 1, it is possible to quantify the rate of residual epoxide group with time (Figure 1). It appears that the half-life (time at which 50% of the

initial epoxide functions are consumed) of the epoxide ring of AGE is about 1h30, and the quasi complete opening of the epoxide ring occurs after 8 hours (90% of the epoxide functions consumed).

$$\%\, residual\ epoxide = 100 * \frac{I_a}{I_f} \quad \text{equation 1}$$

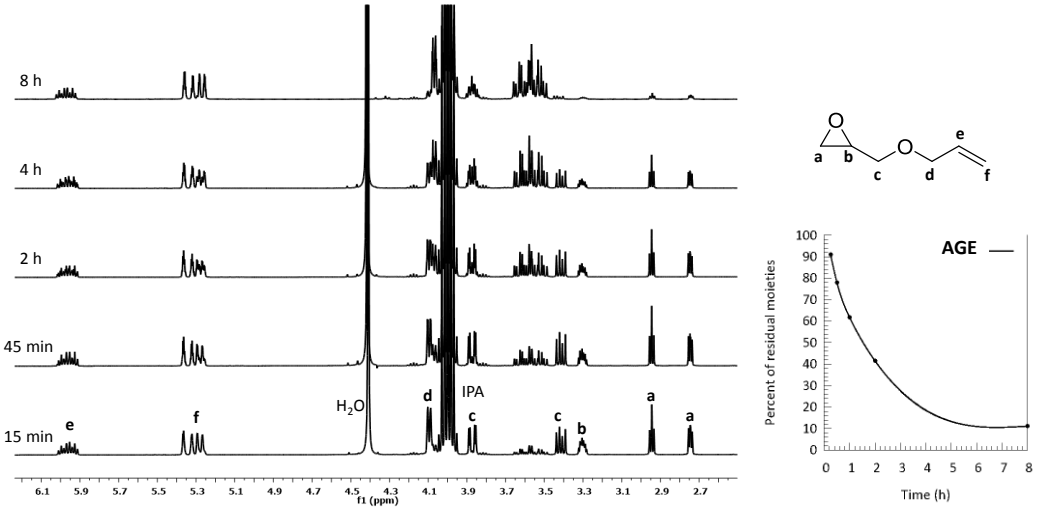

Figure 1. ^{1}H NMR spectra AGE in D_2O/IPA (80/20 w/w), NaOH (0,05 mol.L^{-1}) at 60°C as a function of time, and evolution of the rate of residual epoxide ring with time.

A similar hydrolysis profile was emphasized in the case of propargyl glycidyl ether (Figure **SI.3**), clearly anticipating that the chemical modification of polysaccharides (CMC and XG) with the glycidyl derivatives should not exceed 7 or 8h upon such experimental conditions. Considering this, the reaction of xyloglucan with AGE was first carried out in aqueous basic medium at 60°C using a stoichiometric amount of epoxide and hydroxyl functions, a AGE/NaOH ratio = 3 and a concentration of AGE = 20 gL^{-1}. Raman analysis of the purified modified XG derivative evidences the presence of the absorption band of alkene bond at 1640 cm^{-1} (Figure 2 a). In order to confirm the efficiency of the purification step, a mixture of polysaccharide (CMC or XG) with pre-hydrolysed AGE was prepared and submitted to similar washing procedure and analyzed by Raman analysis (spectra 2 Fig. 2a & 5 Fig. 2b).

No signal at 1640 cm^{-1} was identified on these Raman responses attesting that AGE reactant are not physisorbed and are well covalently attached onto polymer chains.

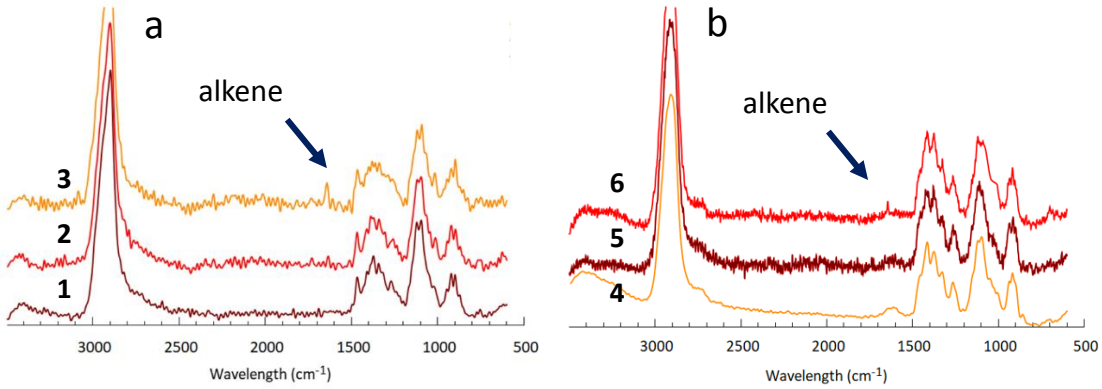

Figure 2. Raman spectra of a) XG and b) CMC (unmodified polysaccharide (spectra 1 & 4), after mixture with hydrolyzed AGE followed by washing step (spectra 2 & 5), and after reaction with glycidyl allyl éther,1 eq/OH at 60 °C, 7h) followed by washing step (spectra 3 & 6)).

^{1}H-NMR analysis also proves the achievement of the ligation, as ^{1}H signals at 5.3 and 6 ppm corresponding to the allyl protons (Ha, and Hb) can be identified onto the spectra of modified XG (Figure 3a). The degree of substitution (DS, calculated as explained in experimental part) over time was quantitatively monitored from the integration of allyl (Ha, and Hb) and anomer protons of the different sugar units (1xy, 1xy', 1gl et 1ga) [50], emerging at respectively 5.13, 4.94 and 4.55 ppm. As shown in Figure 3 b), regarding the allyl functionalization of XG, the DS reaches a plateau at 0.14 after 7 h of reaction.

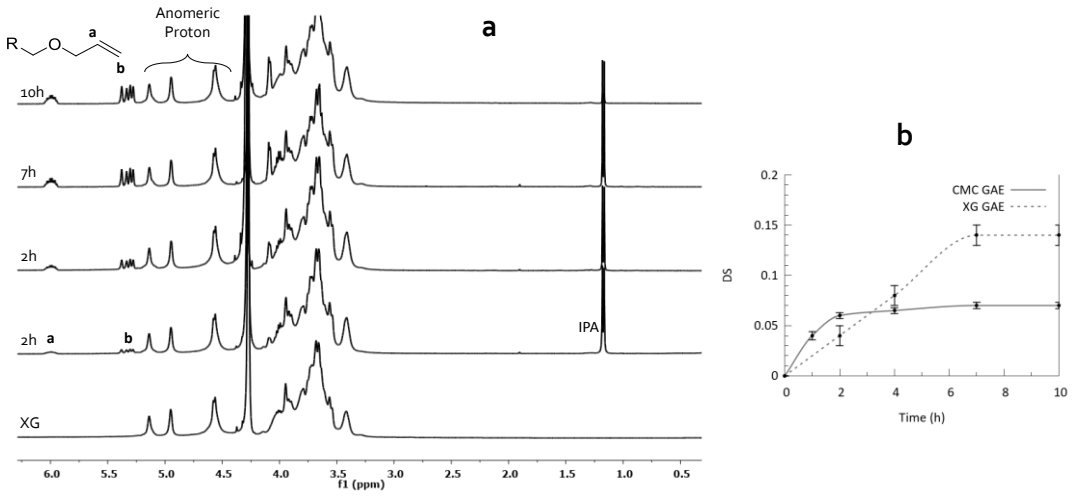

Figure 3. a) ^{1}H-NMR spectra (D_2O, 75°C) of allyl-functionalized XG after different reaction times (1 eq/OH AGE, 0.33 eq/OH NaOH, 60°C); b) Evolution of DS over time for allyl-functionalized XG and CMC.

Different experiments were achieved by using various amounts of AGE and NaOH in order to study their impact on the grafting efficiency. The results, gathered in Table 1, indicate that DS values can be tuned by adjusting the AGE/NaOH ratio while keeping the NaoH/OH ratio constant (0.33 eq/OH; entries 1-4) or by varying both ratios (entries 5-7). A substantial DS values up to 0.54 (entry 7) was obtained with the highest concentrations of reagent and NaOH at 60°C. However, highly functionalized xyloglucans with DS superior to 0.4 exhibit relatively poor water solubility, even at 60°. Interestingly, the functionalization of the polysaccharide can be carried out at low temperatures (30°C, entry 8) or in pure water (entry 9), but at the expense of the grafting efficiency (DS= 0.05 and 0.11 for entries 8 and 9 respectively vs 0.14 for entry 1).

The same chemical strategy was then successfully transposed to CMC (see Table 1, entries 10-18), as also proved by Raman and NMR spectroscopy (Figure 2b and **SI.4**). The DS of the modified CMC derivatives are slightly lower than the ones resulting from the XG modification AGE (DS = 0.34 for CMC vs 0.54 for XG in the same conditions, see entries 7

and 15, Table 1). This lower reactivity also highlighted by the plateau of DS Figure 2b, can

Entry	Polysaccharide	AGE	NaOH (eq/OH)	Ratio	H_2O/IPA	T(°C)	DS

reasonably be ascribed to the steric hindrance caused by the carboxymethyl side groups present onto the polymer backbone, and by the lower concentration of OH groups in CMC, amenable to be converted in allyl functions. To evaluate the general applicability of this straightforward modification procedure, a second functional glydicyl derivative i.e. propargyl glycidyl ether (PGE), was considered for grafting, onto XG and CMC under similar experimental conditions (Table 2). For both XG and CMC, the ligation of alkyne groups was unequivocally underpinned by the appearance of the characteristic signal of alkyne bond at 2115 cm-1 in the Raman spectra of derivatized polymers (Figure **SI.5**).

Table 1. Scope of the reaction for modification of XG, and CMC by allyl glycidyl ether

		(eq/OH)		AGE/NaOH			
1	XG	1	0.33	3	80/20	60	0.14
2	XG	3	0.33	9	80/20	60	0.29
3	XG	6	0.33	18	80/20	60	0.4
4	XG	9	0.33	27	80/20	60	0.43
5	XG	3	1	3	80/20	60	0.29
6	XG	6	2	3	80/20	60	0.44
7	XG	9	3	3	80/20	60	0.54
8	XG	1	0.33	3	80/20	30	0.05
9	XG	1	0.33	3	100/0	60	0.11
10	CMC	1	0.33	3	80/20	60	0.07
11	CMC	3	0.33	9	80/20	60	0.13
12	CMC	6	0.33	18	80/20	60	0.3
13	CMC	3	1	3	80/20	60	0.2
14	CMC	6	2	3	80/20	60	0.3
15	CMC	9	3	3	80/20	60	0.34
16	CMC	1	1	1	80/20	60	0.06
17	CMC	1	0.33	3	80/20	30	0.04
18	CMC	1	0.33	3	100/0	60	0.07

Unfortunately, no alkyne proton could be detected by ^{1}H NMR in D_2O (owing to its acidic character) making the direct estimation of the DS impossible. To evaluate the extent of the modification, we next engaged the alkyne-functionalized polymers in copper alkyne-azide cycloaddition click reactions (CuAAC) with a large excess of PEG azide (11-azido-3,6,9-trioxaundecane-1-amine) in water [43]. Raman analysis collected after the CuAAc coupling, confirmed the full consumption of the alkyne groups and ^{1}H NMR analysis displays the ^{1}H response of the expected triazole ring at 8.1 ppm (Figure **SI.6**). By assuming that the CuAAC coupling is quantitative, alkyne functionalized XG and CMC derivatives with DS ranging from 0.09 to 0.24 and from 0.05 to 0.20 were synthesized (Table 2). The comparison of the DS values obtained upon similar experimental reactional conditions (for instance, entry 5 Table 1 vs entry 2 Table 2 or entry 13 Table 1 vs Entry 4 Table 2) suggests that the reactivities of both, AGE and PGE are roughly similar.

Table 2. Conditions of propargyl glycidyl ether grafting at 60°C in water/IPA (80/20) and degree of the substitution (DS) of the resulting biohybrids.

Entry	Polysaccharide	PGE (eq/OH)	NaOH (eq/OH)	Ratio AGE/NaOH	DS
1	XG	1	0.33	3	0.09
2	XG	3	1	3	0.24
3	CMC	1	0.33	3	0.05
4	CMC	3	1	3	0.20

Aiming at evaluating their reactivity, the allyl-functionalized XG and CMC derivatives were subjected to radical (co)polymerization in aqueous medium with classical comonomers such as acrylamide and sodium acrylate monomers. Due to the high functionality in allyl groups of XG, and CMC, we anticipated that their participation to a copolymerization process in water would give rise to the formation of chemically cross-linked hydrogels. Contrary to acrylamides or acrylates [51], allyl and especially propargyl functions exhibit poor reactivity in radical reactions and to our knowledge the reactivity ratios of AGE and PGE in radical copolymerization systems have not been reported in the literature. However, the reactivity ratios have been estimated for the copolymerization of allyl monomers (A) such as allyl acetate or allyl chloride with n-butyl acrylate (B) [52, 53]. The reactivity ratios reported in these studies, $r_A \ll 1$ and $r_B \gg 1$ (5,8 and 11,7 respectively), indicate that allyl monomers are a priori not suitable for homopolymerization (via free radical polymerization) but can be involved in radical copolymerization/crosslinking procedures with acrylate/acrylamide monomers [54, 55].

A series of copolymerization experiments were performed at 70 °C by mixing allyl-functionalized polysaccharide with a mixture of two co-monomers namely acrylamide and sodium acrylate in water. The gelation phenomena were optically observed. Examples of hydrogels are given in Figure 4.

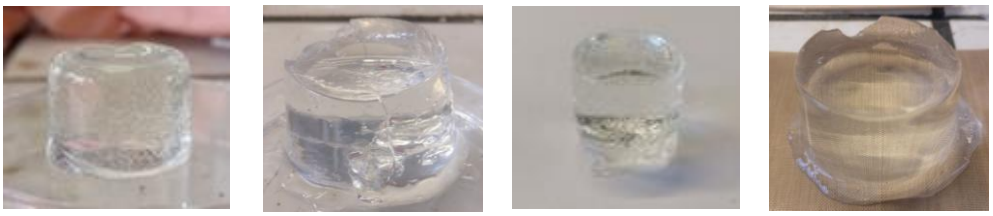

After synthesis After swelling After synthesis After swelling

a) b)

Figure 4. Hydrogels resulting from: a) Allyl-XG with DS_{allyl} = 0.25; and b) Allyl-CMC with DS_{allyl} = 0.13

Table 3. Main characteristics of the hydrogels obtained through free radical polymerization of sodium acrylate, acrylamide and allyl-functionalized XG and CMC derivatives (the weight ratio between polysaccharide/monomers is 50/50).

Entry	Polysaccharide	DS	T_{ex} (%)	SR (g_{water}/g_{gel})
1	XG	0.1	62	390
2	XG	0.25	63	220
3	XG	0.38	56	180
4	CMC	0.06	100	-
5	CMC	0.13	57	1000
6	CMC	0.24	17	270

Contrary to alkyne-functionalized polysaccharides that did not lead to the formation of hydrogels whatever the DS, radical copolymerization carried out with the allyl-functionalized XG or CMC derivatives resulted in self-standing hydrogels which maintain their integrity after swelling in water (Table 3 and Figure 4). Tuning the DS of the allyl-functionalized polymers allowed to modulate the swelling behavior so that hydrogels with a swelling ratio (SR) ranging from 180 to 390 were conveniently prepared by using a DS=0.10 and 0.38, respectively. This trend is coherent because the crosslinking density is expected to increase with the number of reactive chemical functions as reported in the literature [56, 57, 58].

Another key parameter is the chemical nature of the derivatized polysaccharide employed as multi-functional cross-linking reagent. As shown in Table 3 (entry 1 vs entry 5), for a given DS in allyl groups, the hydrogels exhibiting the higher swelling ratios were prepared from allyl-functionalized CMC (SR value of 1000, entry 5, Table 3).

Surprisingly, the extractable rates from the xyloglucan-based hydrogels remained constant at around 60% whatever the DS of the XG derivatives, suggesting that a significant proportion of the grafted allyl functions do not participate to the copolymerization radical process. Conversely, the DS value has a great impact on the features of the hydrogels when allyl-functionalized CMCs are used. Whereas the derivatized CMC with the lowest DS (0.06) fails at generating a hydrogel (Table 3 entry 4), the extractable rate is 57% for DS = 0.13 (Table 3 entry 5) and decreased down to 17% for the DS = 0.24 (Table 3 entry 6). These discrepancies highlight differences in terms of reactivity of allyl functionalized polysaccharide derivatives probably leading to different monomer conversion rates. These changes of reactivity dependently of the nature of polymer chains can be reasonably explained by i) a lower overall mobility of the XG chains due to their significantly higher molecular weight (Mw of 795,000 $g.mol^{-1}$ for XG vs 250,000 $g.mol^{-1}$ for CMC), and to the ramified nature of the XG polysaccharide structure and/or ii) a different chain conformation in aqueous basic medium leading to a different behavior in solution. Indeed, the presence of carboxylate groups onto the CMC backbone at this pH enhances the solubility of CMC in water, favors the CMC chains to adopt a more extended conformation owing to the formation of intra and interchain electrostatic repulsions, which might promote the accessibility of the allyl side-groups for radical reaction. Thus, the generation of hydrogels from the use of allyl-functionalized XG and CMC as cross-linking reagent confirms the ability of the grafted allyl functions to react upon radical conditions in aqueous medium.

Adsorption of functionalized xyloglucan and carboxymethylcellulose onto cellulosic subsrates

As previously mentioned in the introduction, the adsorption of chemically modified polysaccharides appears as a powerful tool for the valorization of cellulosic substrates. This sustainable and simple approach resulting from the physisorption of modified polysaccharides in aqueous medium, is particularly adapted to tailor the surface properties of cellulosic materials without jeopardizing its attractive bulk properties. The interest herein is to impart cellulose surfaces with reactivity conferred by the presence of allyl and alkyne functions along the polymer chains. First, in order to verify the ability of derivatized XG and CMC to be adsorbed onto cellulosic substrate, aqueous solutions of the native and allyl-functionalized XG and CMC (pH ≈ 6) characterized by different DS were sprayed at a concentration of 5 $g.L^{-1}$ (semi-diluted regime since C >> C*) onto two cellulosic substrates, namely a model Whatman paper and wood fibers [59]. Figure 5 gathers the adsorption yield that is to say the percentage of physisorbed product after a washing step.

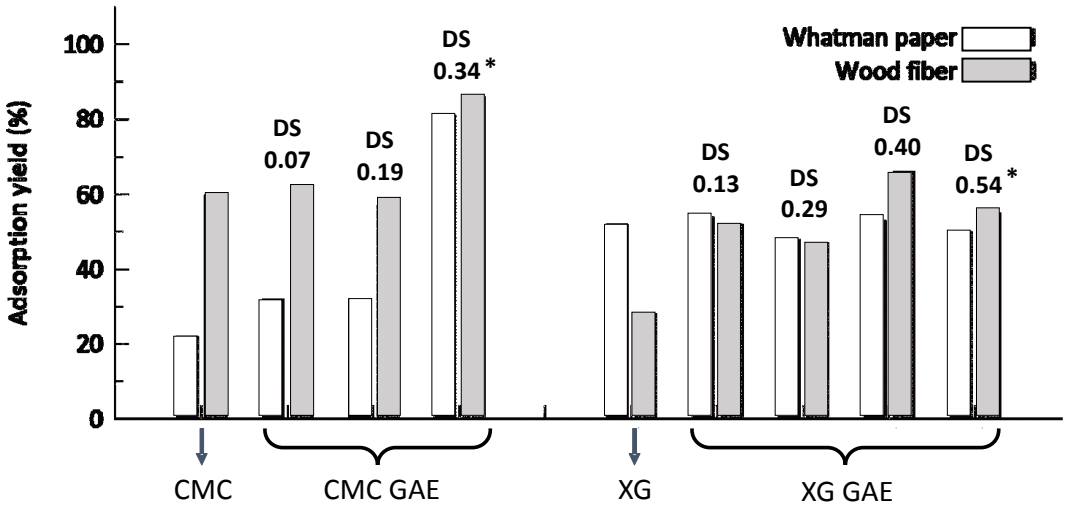

Figure 5. Adsorption yields of allyl-functionalized CMC and XG derivatives, compared to the unmodified polysaccharides (* *Slightly fuzzy aqueous solutions with no decantation with time)*

As shown in Figure 5 (right), the good adsorption propension of XG onto Whatman paper is not altered by the grafting of allyl-functions, as similar adsorption yields around 50 % are obtained, whatever the DS value (from 0.13 up to 0.54). Regarding the adsorption onto wood fibers, the adsorption of native XG chains is less favorable (adsorption yield ~ 30%), and the presence of rather apolar allyl residues onto XG chains promotes the adsorption yields up to 66 % for a DS=0.40. Such polymer adsorption enhancement induced by the modification with allyl functions is consistent with the chemical composition of wood fibers which contain cellulose but also of lignin in high content. In this way, the functionalized XG chains establish not only hydrogen bonds at the interface but also hydrophobic and Van der Waals interactions with cellulose [32] and lignin [60]. Such interactions lead to an entropy gain that derives from the release of water trapped on the surface during adsorption.

Contrary to XG, the adsorption of unmodified CMC is noticeably more pronounced onto wood fibers than onto Whatman paper (~ 20 vs 60 % yields, see Figure 5 left) probably because the electrostatic repulsion is higher with Whatman paper which is slightly oxidized [61]. The allyl functionalization of CMC has a small effect on the adsorption yields onto both substrates at moderate DS values (0.07 and 0.19). For a higher extent of modification (DS = 0.34), the adsorption yield is significantly increased up to 80% onto Whatman paper and 84 % onto wood fibers. The solution of allyl-functionalized CMC of DS = 0.34 is slightly turbid, due to the presence of allyl functions which modifies the solubility parameter of modified CMC. Such an alteration of the solubility can originate from chains aggregation which much probably resulted in a more efficient packing of the adsorbed macromolecules onto the cellulosic surfaces. Moreover, this difference in the adsorption ability could be reasonably explained by the formation or reinforcement of other types of favorable driving forces (Van der Walls, hydrophobic interactions) at the interface with the cellulose substrate caused by the covalent tether of allyl residues. Relatively similar behavior has been previously reported by

Stuart et al. [62] for dodecanyl esters of CMC ($DS_{dodecane}$ = 0.012) which tend to be aggregated in aqueous at pH 4-6 and consequently to be adsorbed onto polystyrene surfaces for which unmodified CMC has no chemical affinity. In this particular example, as mentioned by the authors, the presence of dodecane residues favors the establishment of hydrophobic interactions with polystyrene. The adsorption of alkyne-functionalized XG (DS = 0.09) and CMC (DS = 0.04) was additionally examined (**SI.7**). The behaviors of unmodified XG and alkyne-XG toward Whatman are quite similar. These results are in concordance with data reported by Xu et al. [63] who reported that an alkyne modified xyloglucan (Mw = 17,000 g/mol) (regioselective modification of galactose units by enzymatic oxidation followed by reductive amination with propargylamine) is adsorbed onto Whatman paper in a similar manner to unmodified xyloglucan. It results that for comparable DS, the adsorption ability of alkyne-XG is roughly similar than for allyl-one with comparable adsorption yields, which is consistent with the similarities in terms of chemical composition between the two types of modified derivatives (relatively low DS). The good propensity of alkyne-modified XG to interact with cellulose surfaces will be advantageously exploited to tackle a precise 3D topochemical mapping allowing to image the distribution of the modified polysaccharides at the surface and within the cellulosic substrates through Raman confocal microscopy by collecting the alkyne response used as a specific tag (*vide supra*). In order to gain more insights into the ability of modified polysaccharide derivatives to be adsorbed onto cellulosic substrate and to complete the data achieved by spraying deposition (Figure 5), *in-situ* QCM-D analysis of adsorption were undertaken. For this study, a gold sensor was first covered by a spin-coated poly(allylamine) hydrochloride layer, to provide hydrophilicity, and further coated with a thin layer of CNC. Solutions of XG, and allyl-functionalized XG at 15 $\mu g.mL^{-1}$ in pure water at pH 7 were injected, allowing for depositing the polymers onto the cellulose surface for about 40 minutes. The evolution of $\Delta f_n/n$ and ΔD_n was monitored for native XG,

and modified XG presenting different DS (DS = 0.10, 0.21 and 0.29) as a function of time (Figure 6). For sake of clarity, the variations of frequency and energy dissipation for a single overtone (n = 3) are given to compare the adsorption features of the different samples.

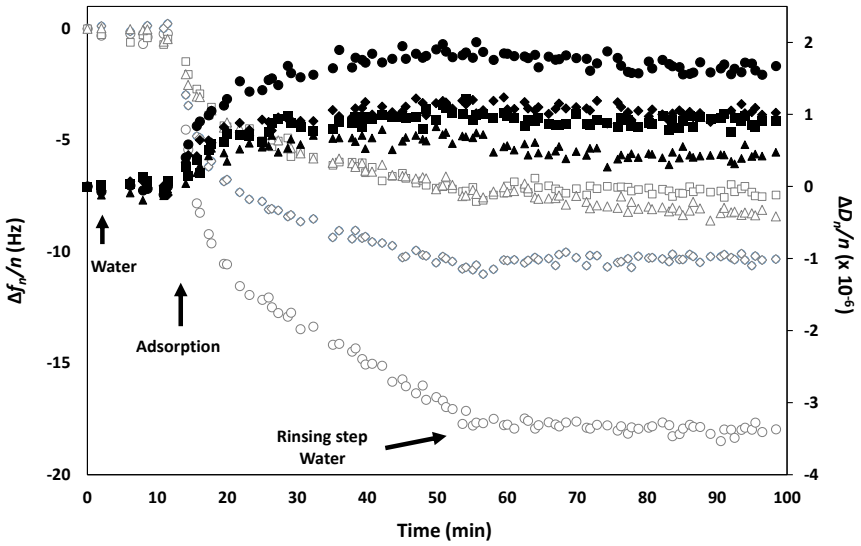

Figure 6. Normalized frequency $\Delta f_n/n$, white symbols) and dissipation (ΔD_n, black symbols) changes for the overtone number n = 3 of the cellulose surfaces, exposed to unmodified XG (○ and ●), and allyl-modified XG with DS=0.10 (◊ and ♦), 0.21 (▲ and Δ), and 0.29 (□ and ■) solutions (15 µg/mL, at pH7, in pure water), as a function of time at 25°C. The arrows indicate the initial baseline (cellulosic substrate in water), the injection of the polymer solutions and the rinsing step (pure water)

Table 4. Δfn/n, ΔD and surface coverage ((Δm in mg/m2), as calculated by the Sauerbrey equation of XG and allyl-XG derivatives (15 µg.mL-1 in pure water). Measurements were performed after adsorption and rinsing with water. Mean values of at least two independent measures (except for entry 3) are indicated.

Entry	Sample	$\Delta f_n/n$ (Hz)	ΔD_n (x 10^{-6})	Δm (mg/m^2)

1	XG	- 16.8 ± 1.8	1.2 ± 0.3	3.0 ± 0.3
2	XG allyle (DS = 0.10)	- 10.6 ± 0.5	1.2 ± 0.2	1.9 ± 0.1
3	XG allyle (DS = 0.21)	- 8.6 ± 0.7	0.4 ± 0.1	1.5 ± 0.2
4	XG allyle (DS = 0.29)	- 6.3 ± 1.1	0.9 ± 0.3	1.1 ± 0.2

The noticeable change of the resonance frequency, induced after each polymer injection, proves that the polymers are adsorbed onto the cellulose surface (Figure 6). More specifically, $\Delta f_n/n$ values (Table 4, Entries 1-4) decreased to -17 Hz for XG and from -10.6, to -6.3 Hz for the substituted XG derivatives, highlighting the effect of the covalent grafting on the adsorption. Moreover, the rinsing step did not lead to any pronounced desorption of the polymer chains, as underpinned by the absence of any noticeable shift of the signals, meaning that the adsorption process is irreversible upon the applied experimental conditions and reflecting the establishment of strong interfacial interactions.

In parallel, the sample injection is accompanied by relatively small dissipation changes (Table 4, Entries 1-4. $\Delta D_n \approx 1 \times 10^{-6}$), which reflects the formation of a relatively rigid and non-viscoelastic layer. [34] In these conditions, the adsorbed mass can be employed to estimate the mass of adsorbed polymers through the Sauerbrey equation (Table 4, Δm). The calculated adsorbed mass, Δm of 3 mg.m^{-2} (entry 1) is closed to the one reported by Eronen *et al.* [64] and Villares *et al.* [65] for XG of high molecular weight adsorbed onto cellulose nanofibrils and cellulose nanocrystals, respectively. By comparing the frequency profiles of XG with those of the modified XG series, an effect of the chemical modification extent is observed. A slower adsorption could be detected for the modified XG (see Δm values, table 4), and this trend is all the more pronounced as the number of allyl residues along the XG backbone is high (entry 2, 3 and 4). Such changes in frequency of resonance reflect that allyl side groups

affect the mode of adsorption of the polysaccharide chains onto the cellulose surface. The presence of allyl moieties might cause steric hindrance along the XG backbone and the substitution of the hydroxyl groups by allyl ones probably impedes and partially impairs the formation of hydrogen bonds at the interface with the cellulose surface. Even if an impact of the functionalization is visible, the adsorption of allyl-XG derivatives remain completely satisfactory. It is tricky to quantitatively compare these results with the adsorption yields values resulting from the titration experiments after spraying, since the concentrations of polysaccharides employed for QCM-D analysis are very low, well below the critical overlap concentration C*. Villares et al. [65] have shown that at a concentration > 6mg.L^{-1}, the XG chain adsorption is fast enough to hamper the rearrangement of the chain, thus favoring the saturation of the cellulose surface with the formation of polymer loops. The lower values of energy dissipation resulting from the deposition of allyl-XG, compared to unmodified XG, indicates a less hydrated character of the deposited layer, caused by the presence of apolar allyl residues which leads to the formation of hydrophobic zones onto the surface and tend to expulse water molecules. Thus, not only the decrease of □m values observed for the allyl-functionalized polymers stems from a modification of the interfacial interactions but also probably originates from a noticeable water molecules exclusion during the adsorption process. The QCM-D analysis of unmodified CMC and allyl-CMC derivatives upon similar experimental conditions revealed that the adsorption onto CNC layers was unfavored and partial desorption occurred with allyl derivatives during the rinsing step (**SI.8.a**). This can be ascribed by the formation of electrostatic repulsions between carboxylate groups of CMC, and partially negatively charged surface of cellulose substrate composed of nanocrystals of cellulose [66]. As reported in literature, the addition of $CaCl_2$ electrolyte is required to promote CMC adsorption onto this kind of cellulosic substrates [67]. Keeping this in mind, we turned to the preparation of a neutral amorphous cellulose surface resulting from the spin-

coating of cotton linters dissolved in dimethylacetamide/LiCl, in order to avoid the potential influence of charge-repulsion effects between CMC backbone and the substrate. In such experimental conditions, the deposited mass Δm after injection of unmodified CMC and allyl derivative (DS = 0.07) are high, between 2.5 and 2.7 mg.m^{-2} and no desorption occurs during the rinsing stage (**SI.8.b**). The dissipation values (ΔD_n) are higher than 3 X10^{-6}, reflecting a higher hydration level of the layer, compared to the XG-based analogous layers. This feature is linked to the very hydrophilic character of CMC conferred by the presence of negatively charged carboxylate groups providing additional intra and interchain repulsive electrostatic interactions which exalts its ability to swell. No noticeable difference in the adsorption response is observed between unmodified CMC and allyl-CMC, which can be related to the low DS value of the derivative, consistently with the titration data onto Whatman papers given in Figure 5. These encouraging results emphasize the possibility to adsorb CMC and its reactive derivatives onto lignocellulosic substrates.

By taking advantage of the well-defined Raman response of alkyne functions (intense signal at around 2115 cm^{-1}) [41], we finally realized a topochemical mapping of alkyne moieties to examine the spatial distribution of the functionalized CMC and XG chains sprayed onto Whatman paper by Raman confocal microscopy. Raman mappings were carried out onto coated whatman papers on a surface of several hundred μm^2 (380x380 μm^2) and at various depth levels with step sizes of 10 μm. As shown in Figure 7 a and c, the Raman images reveal the presence of the expected alkyne signals on the integrality of the surface, confirming that the paper sheet is completely covered with adsorbed CMC/XG chains. However, some disparities and fluctuations in terms of alkyne concentration (more highly and less modified regions in red and yellow) emerge. These intensity gradients much probably stem from the Raman detection, which can be interfered by i) the surface geometric features of the sample impacted by the non-planarity of the substrate, and ii) the heterogeneous deposition of the

polymer chains linked to the use of a lab spray process. Also, the analysed sample was subjected to a drying step, which can generate a roughness able to disrupt the Raman signal, and thus the final detected intensity. To gain insight into the penetration of the polymer chains into the cellulosic substrate, Raman mapping was further carried as a function of the depth. As evidenced in Figures 7b and 7d, the response of the alkyne bonds remains detectable over a thickness ~ 40 µm, i.e. the diameter of one cellulose fiber, whatever the nature of the adsorbed alkyne-functionalized polymer. This diffusion of polysaccharide chains inside the substrate is an advantageous feature to promote the adhesion of the coated layers.

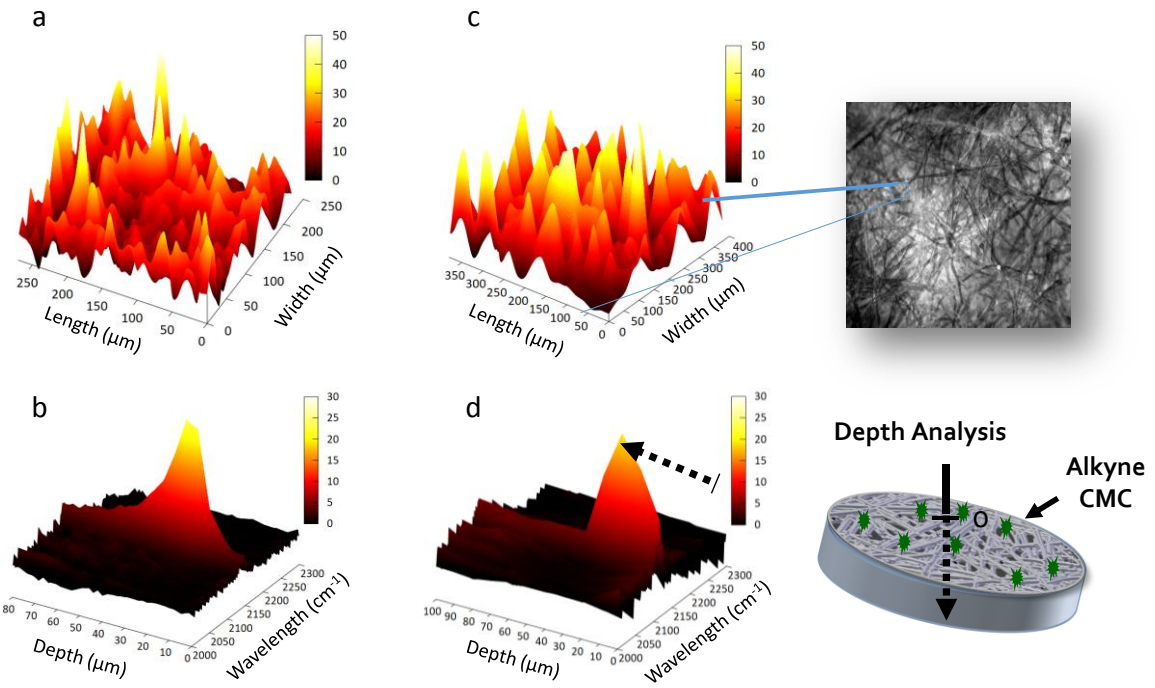

Figure 7. Raman mapping of Whatman paper coated by spraying a solution of alkyne-modified XG (20 g.L^{-1}) of DS = 0.09 in 2D (image a) and in 3D (image b), and of alkyne-CMC of DS = 0.04 in 2D (image c) and 3D (image d). Pictures a and c correspond to the analysis of the Whatman cellulose surface. Pictures b and d characterize the chains diffusion over 40 µm inside the paper.

4. **Conclusion**

Herein, xyloglucan (XG) and carboxymethyl cellulose sodium (CMC) were chemically modified by means of opening reaction with propargyl glycidyl ether and allyl glycidyl ether in basic aqueous medium at low temperature. A deep scrutiny of the reaction parameters showed that the hydrolysis side reaction of the epoxy functions does not hamper the desired ligation and that a modulation of the DS can be reached by playing with the molar ratio of NaOH and reagent. XG is a little more reactive than CMC and allyl and propargyl glycidyl ethers have roughly similar reactivity. The radical copolymerization in water of allyl-derivatives with acrylamide and sodium acrylate led to hydrogel, thus proving the good reactivity of such polysaccharide derivatives. The depositions of XG and CMC on Whatman paper and wood pine fibers by spraying aqueous solutions following by desorption step were confirmed by the significant rise in the adsorbed mass. With allyl-and alkyne-derivatives, the adsorption degrees were similar or higher than the non-derivatives proving that neither the nature of grafting moieties nor the DS alter the deposition. Additional data from QCM-D confirmed that CMC and its derivatives had less affinity with nanocellulose surface because of the electrostatic repulsion whereas the high affinity of XG was slightly reduced with the presence of the apolar allyl residues. Finally, a topochemical mapping with alkyne derivatives highlighted a rather heterogeneous deposition of the polymer chains much probably related to the use of a lab spray process and interestingly polysaccharide chains are able to diffuse inside the cellulosic substrate. Thus, this new strategy allows for modifying the cellulosic surface features in a simple, robust and ecofriendly way and paves the way for the design of new cellulosic materials.

5. Acknowledgements

This work was supported by the “Institut Technologique Forêt Cellulose Bois-Construction Ameublement” (FCBA) in France. The authors are also grateful to Nadège Beury for her

excellent support for the QCM-D data acquisition and to Fernande Da Cruz-Boisson, Carlos Fernández de Alba and Patrick Goetinck for their precious advice in NMR experiments.

References

[1] Farid Chemat, Maryline Abert Vian and Harish Karthikeyan Ravi Current Opinion in Green and Sustainable Chemistry 2021, 28:100450

[2] Ferreira E. S., Rezende C. A., Cranston E. D., Green Chem., 2021, 23, 3542-3568

[3] De Assis T., Reisinger L., Dasmohapatra S., Pawlak J., Jameel H., Pal L., Kavalew D., Gonzalez R. 2018, BioResources 13(3), 6868-6892

[4] Catarina Felgueiras, Nuno G. Azoia, Cidália Gonçalves, Miguel Gama, Fernando Dourado Front. Bioeng. Biotechnol., 2021, 608826

[5] Kargarzadeh H., Ahmad I., Thomas S., Dufresne Handbook of Nano-cellulose and cellulose Nanocomposite Wile-VCH 2017

[6] S.H. Hassan1,2, Lee Hwei Voon1*, T.S. Velayutham2*, Lindong Zhai3, Hyun Chan Kim3 and Jaehwan Kim Journal of Renewable Materials, 2018, 6, No. 1, 1-25

[7] M. Jorfi, E.J. Foster, Journal of Applied Polymer Science, 2015, 132, 41719

[8] D. Klemm, B. Heublein, H.-P. Fink, A. Bohn, Angewandte Chemie International Edition, 2005, 44, 3358-3393

[9] Roy D., Semsarilar M., Guthrie J. T., Perrier S. Chemical Society Reviews, 2009, 38, 2046-2064

[10] Kelechukwu N. Onwukamike, Stéphane Grelier, Etienne Grau, Henri Cramail, Michael A.R. Meier ACS Sustainable Chem. Eng. 2019, 7, 2, 1826–1840

[11] Chang C.-W., Lu K.T. Journal of applied polymer science, 2010, 115, 2197–2202

[12] Maurin V., Bessieres J., Croutxe-Barghorn C., Allonas X., Merlin A. & Masson E.

Cellulose Chemistry and Technology, 2012, 46, 471-476

[13] Arumughan V., Nypel T., Hasani M., Larsson A., Advances in Colloid and Interface Science, 2021, 298, 102529

[14] Littunen K., Kilpeläinen P., Junka K., Sipponen M., Master E. R. & Seppälä J. Biomacromolecules, 2015, 16, 1102-1111

[15] Zhou Q., Rutland M., Teeri T. & Brumer H. Cellulose, 2007, 14, 625-641

[16] Filpponen I., Kontturi E., Nummelin S., Rosilo H., Kolehmainen E., Ikkala O., Laine J. Biomacromolecules 2012, 13, 736-742

[17] Niegelhella K., Chemellic A., Hobischd J., Griessere T., Reiterb H., Hirna U., Spirka S. Carbohydrate Polymers, 2018, 179, 290-296

[18] Deutschlea A.L., Römhildb K., Meisterb F., Janzonc R., Riegert C., Saakec B. Carbohydrate Polymers, 2014, 102, 627-635

[19] Nordgren N., Eronen P., Österberg M., Laine J., Rutland M.W. Biomacromolecules 2009, 10, 3, 645-650

[20] Pan Y., Xiao H. Song Z. Cellulose, 2013, 20, 485–494

[21] Alexakis A.E., Engström J., Stamm,A., Riazanova A.V., Brett C. J. , Roth S. V., Syrén P. O., Fogelström L., Reid M. S., Malmström E., Green Chem., 2021, 23, 2113-2122

[22] Grigoray O., Wondraczek H., Pfeifer A., Fardim P., Heinze T. ACS Sustainable Chem. Eng. 2017, 5, 1794-1803

[23] Pettignano A., Moreau C., Cathala B., Charlot A., Fleury E. ACS Sustainable Chemistry & Engineering 2019, 7, 14685-14697

[24] Grantham N. J., Wurman-Rodrich J., Terrett O. M., Lyczakowski J. J., Stott K., Iuga D., Simmons T. J., Durand-Tardif M., Brown S. P., Dupree R., Busse-Wicher M., Dupree P. Nature Plants, 2017, 3, 859-865

[25] Kôhnke T., Pujolras C., Roubroeks J. P., Gatenholm P., Cellulose, 2008, 15, 537

[26] Berglund J., Kishani S, Morais de Carvalho D., Lawoko M., Wohlert J., Henriksson G., Lindström M. E., Wågberg L., Vilaplana F. ACS Sustainable Chemistry and Engineering, 2020, 8, 10027-10040

[27] Fry S. C. Journal of Experimental Botany 1989, 40, 1-11

[28] Wolfgang G. Glasser, G. Ravindran, Rajesh K. Jain, Gamini Samaranayake, Jason Todd Biotechnol. Prog. 1995, 11, 552-557

[29] Estelle Doineau, Guillaume Bauer, Léo Ensenlaz, BrunoNovales, CécileSillard, Jean-Charles Bénézeta, Julien Bras, Bernard Cathala, Nicolas Le Moigne Carbohydrate Polymers 2020, 248, 116713

[30] Dammak A., Quémener B., Bonnin E., Alvarado C., Bouchet B., Villares A., Moreau C., Cathala B. Biomacromolecules 2015, 16, 589-596

[31] Stiernstedt J., Brumer H., Zhou Q., Teeri T. T., Rutland M. W. Biomacromolecules 2006, 7, 2147-2153

[32] Benselfelt T., Cranston E. D., Ondaral S., Johansson E., Brumer H., Rutland M. W., Wågberg L. Biomacromolecules 2016, 17, 2801-2811

[33] Zhao Z., Crespi V. H., Kubicki J. D., Cosgrove D. J., Zhong L. Cellulose 2014, 21, 1025-1039

[34] Hanus J., Mazeau K. Biopolymers 2006, 82, 59-73

[35] Lopez M., Bizot H., Chambat G., Marais M. F., Zykwinska A., Ralet M.-C., Driguez H., Buléon A. Biomacromolecules 2010, 11, 1417-1428

[36] Villares A., Bizot H., Moreau C., Rolland-Sabaté A., Cathala B. Carbohydrate Polymers 2017, 157, 1105-1112

[37] Lowe A.B. Polymer Chemistry, 2010, 1, 17-36

[38] X. Meng, K. J. Edgar Progress in Polymer Science, 2016, 53, 52-85

[39] M. V.Dobrynin, V. Y. Kukushkin, R. M. Islamova Carbohydrate Polymers 2020, 241, 116327

[40] Kokoro Iio, Kentaro Kobayashi, Mutsuo Matsunaga Polym. Adv. Technol. 2007, 18, 953-958

[41] Lijian Sun, Guifa Xiao, Xueren Qian, Xianhui An Carbohydrate Polymers 2019, 207, 68-78

[42] Deng S. Binauld S., Mangiante G., Frances J.M., Charlot A., Bernard J., Zhou X., Fleury E. Carbohydrate Polymers, 2016, 151, 899-906

[43] Mangiante G., Alcouffe P., Burdin B., Gaborieau M., Zeno E., Petit-Conil M., Bernard J., Charlot A., Fleury E. Biomacromolecules 2013, 14,254-263

[44] Huijbrechts A. A., Huang J., Schols H. A., Van Lagen B., Visser G. M., Boeriu C. G., Sudhölter E. J. Journal of Polymer Science Part A : Polymer Chemistry 2007, 45, 2734-2744

[45] Nurmi L., Salminen R., Setälä H. Carbohydrate research 2015, 404, 63-69

[46] Qi H., Liebert T., Heinze T. Cellulose 2012, 19, 925-932

[47] Lawal O. S., Yoshimura M., Fukae R., Nishinari K. Colloid and Polymer Science 2011, 289, 1261-1272

[48] Nielsen T. T., Wintgens V., Amiel C., Wimmer R., Larsen K. L. Biomacromolecules 2010, 11, 1710-1715

[49] Bigand V., Pinel C., Da Silva Perez D., Rataboul F., Huber P., Petit-Conil M. Carbohydrate Polymers 2011, 85, 138-148

[50] Arruda I. R., Albuquerque P. B., Santos G. R., Silva A. G., Mourão P. A., Correia M. T., Vicente A. A., Carneiro-da Cunha M. G. International journal of biological macromolecules 2015, 73, 31-38

[51] Cabaness W., Lin T., Parkanyi C. Journal of Polymer Science Part A: Polymer Chemistry 1971, 9, 2155-2170

[52] Heatley F., Lovell P. A., McDonald J. European polymer journal 1993, 29, 255-268

[53] Brandrup J., Immergut E., Grulke E. A. "Polymer handbook. 4th." Edn. New York : A Wiley-Interscience publication, 1999

[54] Duanmu J., Gamstedt E. K., Rosling A. Starch-Stärke 2007, 59, 523–532

[55] Pohjanlehto H., Setälä H., Kammiovirta K., Harlin A. Carbohydrate research 2011, 346, 2736-2745

[56] Bencherif S. A., Srinivasan A., Horkay F., Hollinger J. O., Matyjaszewski K., Washburn N. R. Biomaterials 2008, 29, 1739-1749

[57] Kim S.-H., Chu C.-C. Journal of Biomedical Materials Research Part A 2000, 49 , 517-527

[58] Reis A. V., Cavalcanti O. A., Rubira A. F., Muniz E. C. International Journal of Pharmaceutics 2003, 267, 13-25

[59] François Muller, Bruno Jean, Patrick Perrin, Laurent Heux, François Boué, Fabrice Cousin Macromol. Chem. Phys. 2013, 214, 2312-2323

[60] Barakat A., Winter H., Rondeau-Mouro C., Saake B., Chabbert B., Cathala B. Planta 2007, 226, 267

[61] Henniges U., Potthast A. Restaurator, 2009, 294-320

[62] Stuart M. C., Fokkink R., Van der Horst P., Lichtenbelt J. T. Colloid & Polymer Science 1998, 276, 335-341

[63] Xu C., Spadiut O., Araújo A. C., Nakhai A., Brumer H. ChemSusChem 2012, 5, 661-665

[64] Eronen P., Junka K., Laine J. & Österberg M. BioResources 2011, 6, 4200-4217

[65] Villares A., Moreau C., Dammak A., Capron I., Cathala B. Soft Matter 2015, 11, 6472-6481

[66] Kargl R., Mohan T., Bracic M., Kulterer M., Doliška A., Stana-Kleinschek K., Ribitsch V. Langmuir 2012, 28, 11440-11447

[67] Orelma H., Teerinen T., Johansson L.-S., Holappa S., Laine J. Biomacromolecules 2012, 13, 1051-1058